2.A.1:
3.A

Nuclear Physics **A323** (1979) 253–270; © *North-Holland Publishing Co., Amsterdam*

GAMMA-RAY STRENGTH FUNCTIONS FOR A = 70–90 NUCLEI

G. SZEFLINSKA, Z. SZEFLIŃSKI and Z. WILHELMI

Institute of Experimental Physics, University of Warsaw, Poland

Received 1 March 1979

Abstract: The radiative proton capture reaction has been used to study the energy dependence of the E1 γ-ray strength function for A = 70–90 nuclei in the region between 6 and 10 MeV. Using a Ge(Li) detector, γ-ray spectra of primary radiative transitions have been measured in order to obtain γ-ray intensities averaged over many neighbouring resonances. The γ-ray strength functions were deduced for decay to the levels with well-known J^{π} values. The values of the γ-ray strength function, in the energy region investigated, are well described by a Lorentzian curve extrapolated from the giant resonance region.

E | NUCLEAR REACTIONS ^{70,72,74}Ge(p, γ), ^{84,86,88}Sr(p, γ), ^{89}Y(p, γ), E = 2–3 MeV; measured E_{γ}, I_{γ}. ^{71,73,75}As, ^{85,87,89}Y, ^{90}Zr deduced γ-ray strength functions. Enriched targets, Ge(Li) detector.

1. Introduction

In recent years great progress has been made in giant multipole resonance research. Among other things, isoscalar and isovector giant quadrupole resonances have been discovered, and experimental data have been obtained which point to the existence of the giant monopole resonance.

These interesting discoveries have not, however, stopped us from keeping in mind giant dipole resonances, which have been known for 30 years, and they have even stimulated research in that field. An important role is played here by the measurements of averaged radiation widths and related γ-ray strength functions [1]). The latter quantity being an average value, finds wide application in the description of γ-ray absorption and emission processes and it is particularly useful in cases when the description of a nuclear process requires the use of level density instead of single nuclear levels.

In the recent years a number of surveys [2–4]) have been devoted to γ-ray strength function studies, proving that these problems attract continued interest. The picture they sketch has serious gaps. Especially the problem of the dependence of γ-ray strength functions on the transition energy is far from clear. The knowledge of the 6–10 MeV energy region is particulary scanty, although it is very significant for understanding and describing the important process of nucleon capture. The E1 high energy γ-transitions observed in such a process are sometimes interpreted under the assumption made by Axel [5]) that they are due to the same processes as the giant dipole resonance of Lorentzian shape occuring in photonuclear reactions. Nucleon capture and the photonuclear reaction are reverse processes. Therefore the above assumption has to be complemented by another one, usually referred to as the Brink hypothesis [6]), which states that a giant resonance of universal shape is built on every excited state, which means that the γ-ray strength function is independent of the excitation energy but depends on the energy of the considered γ-transition.

The Brink-Axel hypothesis finds its justification in theoretical considerations. From calculations performed in terms of the quasiparticle-phonon model [7,8]), it follows that the strength function extrapolation made by Axel from the region of the giant resonance maximum to low energies is correct, whereas the hydrodynamical model provides strong arguments supporting Brink hypothesis [9]).

It deserves stating, however, that the discussed assumptions require also an experimental verification in view of their fundamental significance for describing radiation processes. This verification can be provided by measurements of high energy γ-ray spectra from proton capture reactions; by analysing such spectra we can determine the γ-ray strength function for transitions from the 6–10 MeV energy range.

In the present work use has been made of the so-called averaged resonance spectroscopy applied for the first time by Bollinger and Thomas [10]). They have shown that the intensities of high energy primary γ-transitions from the compound nucleus formed as a result of neutron capture to a particular final state, when averaged over many neighbouring resonances in the compound nucleus, depend only on the transition energies and on the spin and parity of that final state. Knowing the energy dependence of such averaged intensities we can determine the unknown spins and parities of the low-lying states. This method has been successfully used both for (n, γ) [10]) and (p, γ) [11–15]) reactions. When the quantum characteristics of the levels populated in the considered γ-transitions are known, we can reverse the procedure and determine from the measured primary spectra of γ-transitions not the spins, but the values of the γ-ray strength function as well as study its dependence on transition energy.

In studies of the γ-ray strength function, the Porter-Thomas fluctuations [16]) play an important role, since the strength function is a quantity proportional to the average partial radiation width $\bar{\Gamma}_\gamma$. The distribution of individual widths Γ_γ is a χ^2 distribution with one degree of freedom, as a consequence of which we get a high value of the dispersion:

$$\langle(\Gamma_\gamma - \bar{\Gamma}_\gamma)^2\rangle = 2\bar{\Gamma}^2. \tag{1}$$

If the value of $\bar{\Gamma}_\gamma$ is determined in a measurement involving n states in the averaging region, then we can estimate the uncertainty in the radiation widths as

$$\Delta\bar{\Gamma}_\gamma = \sqrt{2/n}\,\bar{\Gamma}_\gamma. \tag{1a}$$

This formula enables us to make the contribution of the Porter-Thomas fluctuations as low as required by choosing the width of the averaging interval (and n-value at the same time) on the basis of level density data.

When studying the γ-ray strength function in a nucleon capture experiment, the so-called "high resolution method" suggests itself, consisting in the detection of the particular γ-transitions with high resolution [2]). This method demands that the Porter-Thomas fluctuations be small, and this condition can be fulfilled by averaging the measured transition intensity over many neighbouring resonances. When this method is used for the (p, γ) reaction, it is necessary to use in the experiment a target of small thickness not exceeding a dozen or so keV, so the high resolution of Ge(Li) detector can be taken advantage of.

The cross sections for the (p, γ) reaction are easy to measure for target nuclei with mass number $A < 90$. Reduction of the contribution due to the Porter-Thomas fluctuation can be expected only for nuclei with level density $\rho > 10^3$ MeV^{-1} at excitation energy $E = 10$ MeV, which means that the condition $A > 60$ should be fulfilled. The theoretical analysis of the reaction becomes much simpler when reaction channels other than the radiation one are closed.

2. Experimental procedure

In studies of γ-ray strength functions extracted from proton capture experiments, the mass region $A = 70$–90 is of particular interest. For this region the data regarding the strength function are only fragmentary and come from photo-absorption cross section measurements in the giant resonance region, but there is much information regarding the radiation widths of states produced in the neutron capture reaction. For our studies of the (p, γ) reaction we chose germanium, strontium and yttrium isotopes as targets (see table 1). The available data regarding the structure of low-lying states of the final nuclei produced in such reactions are relatively rich; moreover, the chosen target isotopes reveal a high negative Q-value for the (p, γ) reaction $Q_{p,n} < -3.5$ MeV, which is of practical importance.

TABLE 1

The targets used in the radiative proton capture reaction studies

Isotope	Enrichment (%)	Target thickness (μg/cm^2)	Target thickness (keV) ($E_p = 3$ MeV)
^{70}Ge	96.2	150±12	9.3±0.8
^{72}Ge	98.2	200±12	12.4±0.8
^{74}Ge	98.8	148±11	9.2±0.7
^{84}Sr	68.7	280±40	15.7±2.2
^{86}Sr	95.8	220±20	11.3±1.1
^{88}Sr	99.9	280±20	15.7±1.1
^{89}Y	100.0	250±20	13.7±1.1

TABLE 2

Characteristics of the reactions studied and the measured cross sections for the $\langle\sigma_{p,\gamma_0}\rangle$ reaction

Reaction	Energy range (MeV)	$\langle\sigma_{p,\gamma_0}\rangle$ (mb)	Average excitation energy E_γ (MeV)
^{70}Ge(p, γ)^{71}As	3.0–3.9	17±2	8.0
^{72}Ge(p, γ)^{73}As	3.0–3.9	15±2	9.1
^{74}Ge(p, γ)^{75}As	2.2–2.8	14±2	9.4
^{84}Sr(p, γ)^{85}Y	2.8–3.8	7±1	7.8
^{86}Sr(p, γ)^{87}Y	2.8–3.8	20±2	9.1
^{88}Sr(p, γ)^{89}Y	2.8–3.8	50±5	10.4
^{89}Y(p, γ)^{90}Zr	2.2–3.4	17±3	11.1

TABLE 3

Relative level population intensities and strength functions for ^{71}As

Level energy E_k (keV)	J^π	Ref.	Relative intensities I/I_0	$f_{kλ}$ (10^{-8} MeV^{-3})
0	$\frac{5}{2}^-$	15, 18)	1.000±0.052	5.46±0.28
143	$\frac{3}{2}^-$	15, 19)	1.350±0.081	5.16±0.31
147	$\frac{3}{2}^-$	15, 19)	1.350±0.081	5.16±0.31
508	$\frac{5}{2}^-$	15)	0.711±0.052	3.97±0.29
831	$\frac{3}{2}^-$	15, 18)	0.860±0.052	4.18±0.25
871	$\frac{5}{2}^-$	15, 20)	0.570±0.037	4.40±0.28
990			0.411±0.043	
994	$\frac{3}{2}^-$	15, 18)	0.849±0.052	4.58±0.28
1008	$\frac{5}{2}^+$	15)	0.647±0.041	4.45±0.28
1132	$\frac{5}{2}^+$	15, 18)	0.606±0.043	4.40±0.31
1247	$\frac{3}{2}^-$	15, 20)	0.690±0.048	4.16±0.29
1416	$\frac{3}{2}^-$	15, 18)	0.556±0.041	3.62±0.27
1446			0.442±0.031	
1469	$\frac{3}{2}^-$	15)	0.622±0.041	4.14±0.27
1493			0.382±0.035	
1537	$\frac{1}{2}^+$	15, 18)	0.368±0.031	3.85±0.32
1613 [a])			0.727±0.048	
1702			0.279±0.029	
1735	$\frac{7}{2}^+$	15)	0.172±0.027	4.14±0.65
1758			0.409±0.035	
1831	$\frac{5}{2}^+$	15)	0.355±0.031	3.56±0.31
1853	$\frac{5}{2}^+$	15)	0.351±0.031	3.51±0.30

[a]) Unresolved levels.

The targets were made of separated, enriched isotopes by evaporating them onto 0.2 mm thick tantalum discs. Simultaneously, in an identical geometry, the isotopes were similarly evaporated onto thin aluminium discs in order to allow further determination of the target thickness. Prior to removing the targets from the vacuum system they were coated with a gold layer ($\approx$ 25 μg/cm^2) to prevent oxidation of the evaporated isotopes.

TABLE 4

Relative level population intensities and strength functions for ^{73}As

Level energy E_k (keV)	J^π	Ref.	Relative intensities I/I_0	$f_{k\lambda}$ (10^{-8} MeV^{-3})
0	$\frac{3}{2}^-$	[15, 21, 22]	1.000 ± 0.035	7.81 ± 0.27
67	$\frac{5}{2}^-$	[15, 21, 22]	0.530 ± 0.038	9.18 ± 0.65
84	$\frac{3}{2}^-$	[15, 22, 23]	0.963 ± 0.042	7.73 ± 0.34
254	$\frac{1}{2}^-$	[15, 22, 23]	0.631 ± 0.034	7.89 ± 0.42
394	$\frac{3}{2}^-$	[15, 22, 23]	0.815 ± 0.035	7.27 ± 0.31
428	$\frac{9}{2}^+$	[15, 21–23]	0.080 ± 0.022	9.59 ± 2.65
510	$\frac{5}{2}^+$	[15, 21–23]	0.397 ± 0.028	6.82 ± 0.48
577 [a]			0.856 ± 0.044	
656	$\frac{1}{2}^-$	[15, 22, 23]	0.504 ± 0.033	7.24 ± 0.47
769			0.463 ± 0.040	
857 [a]			0.535 ± 0.035	
886	$\frac{1}{2}^+$	[15, 21]	0.485 ± 0.028	7.74 ± 0.43
894	$\frac{7}{2}^-$	[15, 22]	0.174 ± 0.041	5.50 ± 1.29
1082 [a]			0.730 ± 0.040	
1190	$\frac{3}{2}^-$	[15]	0.401 ± 0.034	5.46 ± 0.40
1216 [a]			0.980 ± 0.044	
1302 [a]			0.724 ± 0.040	
1324	$\frac{5}{2}^+$	[22]	0.347 ± 0.034	8.04 ± 0.78
1344	$\frac{7}{2}^-$	[15, 22]	0.176 ± 0.035	6.35 ± 1.26
1540			0.246 ± 0.022	

[a]) Unresolved levels.

TABLE 5

Relative level population intensities and strength functions for ^{75}As

Level energy E_k (keV)	J^π	Ref.	Relative intensities I/I_0	$f_{k\lambda}$ (10^{-8} MeV^{-3})
0	$\frac{3}{2}^-$	[15, 24]	1.000 ± 0.030	9.28 ± 0.28
199	$\frac{1}{2}^-$	[15, 24, 25]	0.718 ± 0.029	8.73 ± 0.35
265	$\frac{3}{2}^-$	[15, 24, 25]	0.837 ± 0.035	8.46 ± 0.35
279	$\frac{5}{2}^-$	[15, 24, 25]	0.298 ± 0.023	12.11 ± 0.93
304	$\frac{9}{2}^+$	[15, 24, 25]	0.022 ± 0.013	5.27 ± 3.12
401	$\frac{5}{2}^+$	[15, 24, 25]	0.274 ± 0.016	6.69 ± 0.39
469	$\frac{1}{2}^-$	[24, 25]	0.535 ± 0.030	7.11 ± 0.40
573	$\frac{5}{2}^-$	[15, 24, 25]	0.256 ± 0.017	11.47 ± 0.76
619	$\frac{3}{2}^-$	[24, 25]	0.587 ± 0.032	10.11 ± 0.55
822	$\frac{7}{2}^+$	[15]	0.028 ± 0.017	7.42 ± 4.50
861	$\frac{1}{2}^+$	[15, 24, 25]	0.452 ± 0.025	8.73 ± 0.48
886	$\frac{7}{2}^-$	[15]	0.099 ± 0.014	6.50 ± 0.92
1044	$\frac{7}{2}^+$	[15, 25]	0.029 ± 0.017	8.31 ± 4.87
1075	$\frac{3}{2}^-$	[15, 24, 25]	0.513 ± 0.025	6.85 ± 0.33
1129	$\frac{1}{2}^-$	[15, 25]	0.421 ± 0.021	7.05 ± 0.35
1204	$\frac{3}{2}^-$	[24, 25]	0.419 ± 0.022	5.86 ± 0.31
1264			0.221 ± 0.021	
1351	$\frac{3}{2}^-$	[15, 24]	0.451 ± 0.024	6.67 ± 0.35
1371	$\frac{7}{2}^-$	[15, 25]	0.064 ± 0.021	5.01 ± 1.64
1433	$\frac{3}{2}^-$	[15, 24]	0.447 ± 0.024	6.81 ± 0.36
1504	$\frac{3}{2}^+$	[15, 24]	0.205 ± 0.023	5.52 ± 0.62
1606	$\frac{3}{2}^-$	[15, 24]	0.442 ± 0.025	7.20 ± 0.41
1874	$\frac{3}{2}^-$	[15, 24]	0.341 ± 0.030	6.17 ± 0.54
2069	$\frac{3}{2}^-$	[15]	0.297 ± 0.023	5.81 ± 0.45
2102 [a]			0.421 ± 0.038	

[a]) Unresolved levels.

TABLE 6

Relative level population intensities and strength functions for ^{85}Y

Level energy E_k (keV)	J^π	Ref.	Relative intensities I/I_0	f_{kl} (10^{-8} MeV^{-3})
0	$\frac{1}{2}^-$	[14,26]	1.000 ± 0.040	6.25 ± 0.25
18	$\frac{9}{2}^+$	[14,26]	0.093 ± 0.035	4.74 ± 1.79
272	$\frac{5}{2}^-$	[14,26]	0.487 ± 0.045	5.52 ± 0.51
414	$\frac{3}{2}^-$	[14,26]	0.870 ± 0.076	4.85 ± 0.42
436	$\frac{5}{2}^+$	[14,26]	0.429 ± 0.061	4.62 ± 0.65
640	$\frac{3}{2}^-$	[14,26]	0.782 ± 0.042	4.78 ± 0.26
752			0.593 ± 0.042	
796	$\frac{3}{2}^+$	[14,26]	0.632 ± 0.031	4.62 ± 0.23
885	$\frac{5}{2}^+$	[14,26]	0.367 ± 0.050	4.17 ± 0.65
936	$\frac{3}{2}^-$	[14,26]	0.618 ± 0.049	4.29 ± 0.34
966	$\frac{3}{2}^-$	[14,26]	0.705 ± 0.053	4.96 ± 0.37
1215			0.443 ± 0.036	
1281			0.436 ± 0.045	
1379	$\frac{1}{2}^+$	[26]	0.467 ± 0.055	4.75 ± 0.56
1392 [a]			0.654 ± 0.060	
1433	$\frac{3}{2}^-$	[14]	0.461 ± 0.065	4.01 ± 0.57
1605	$\frac{5}{2}^+$	[14,26]	0.226 ± 0.046	4.09 ± 0.83
1676			0.178 ± 0.051	
1726			0.163 ± 0.051	
1820			0.226 ± 0.034	
1846	$\frac{1}{2}^+$	[26]	0.240 ± 0.123	3.07 ± 1.57
1959			0.175 ± 0.046	
2003	$\frac{3}{2}^-$	[14,26]	0.331 ± 0.052	3.82 ± 0.60
2023			0.175 ± 0.046	

[a]) Unresolved levels.

TABLE 7

Relative level population intensities and strength functions for ^{87}Y

Level energy E_k (keV)	J^π	Ref.	Relative intensities I/I_0	f_{kl} (10^{-8} MeV^{-3})
0	$\frac{1}{2}^-$	[13,27,28]	1.000 ± 0.040	5.40 ± 0.21
380	$\frac{9}{2}^+$	[27,28]	0.074 ± 0.005	4.59 ± 0.31
793	$\frac{5}{2}^-$	[27,28]	0.376 ± 0.017	4.78 ± 0.21
983	$\frac{3}{2}^-$	[27,28]	0.632 ± 0.016	4.15 ± 0.11
1152	$\frac{5}{2}^+$	[13,27]	0.270 ± 0.009	4.86 ± 0.16
1184			0.718 ± 0.024	
1407 [a]			0.037 ± 0.011	
1628	$\frac{1}{2}^-$	[13]	0.407 ± 0.013	3.88 ± 0.13
1708			0.239 ± 0.013	
1756			0.127 ± 0.010	
1803	$\frac{5}{2}^-$	[28]	0.156 ± 0.013	2.93 ± 0.24
1848	$\frac{3}{2}^-$	[27,28]	0.271 ± 0.010	2.50 ± 0.09
1981	$\frac{7}{2}^-$	[13]	0.058 ± 0.010	1.81 ± 0.31
2082 [a]			0.474 ± 0.024	
2214	$\frac{3}{2}^+$	[13]	0.216 ± 0.016	2.94 ± 0.22
2292	$\frac{1}{2}^+$	[13]	0.163 ± 0.012	2.83 ± 0.21
2403			0.233 ± 0.014	
2444			0.082 ± 0.010	
2500			0.087 ± 0.010	
2576 [a]			0.261 ± 0.013	
2618	$\frac{3}{2}^-$	[13]	0.219 ± 0.013	2.83 ± 0.17

[a]) Unresolved levels.

TABLE 8

Relative level population intensities and strength functions for ^{89}Y

Level energy E_k (keV)	J^π	Ref.	Relative intensities I/I_0	f_{kl} (10^{-8} MeV^{-3})
0	$\frac{1}{2}^-$	[12, 31, 32]	1.000 ± 0.018	8.30 ± 0.15
809	$\frac{9}{2}^+$	[12, 30–32]	0.124 ± 0.007	8.49 ± 0.47
1508	$\frac{3}{2}^-$	[12, 30–32]	0.826 ± 0.018	6.14 ± 0.14
1745	$\frac{5}{2}^-$	[12, 30–32]	0.384 ± 0.012	5.86 ± 0.19
2225	$\frac{5}{2}^+$	[12, 30, 32]	0.254 ± 0.012	4.69 ± 0.22
2531	$\frac{7}{2}^+$	[12, 30, 32]	0.056 ± 0.017	3.95 ± 1.20
2628	$\frac{9}{2}^+$	[12, 29, 31, 32]	0.025 ± 0.009	3.15 ± 1.13
2687	$\frac{9}{2}^+$	[12]	0.019 ± 0.009	2.45 ± 1.16
2880	$\frac{3}{2}^-$	[12, 30]	0.308 ± 0.013	3.81 ± 0.16
3067	$\frac{3}{2}^-$	[12, 29, 32]	0.247 ± 0.019	3.30 ± 0.25
3105	$\frac{5}{2}^+$	[12]	0.128 ± 0.012	3.34 ± 0.31
3139	$\frac{5}{2}^-$	[32]	0.104 ± 0.015	2.75 ± 0.40
3248	$\frac{3}{2}^+$	[12]	0.179 ± 0.012	3.30 ± 0.22
3410	$\frac{7}{2}^+$	[12]	0.023 ± 0.009	2.33 ± 0.90
3450	$\frac{7}{2}^-$	[12]	0.075 ± 0.008	3.86 ± 0.41
3502	$\frac{3}{2}^-$	[12]	0.180 ± 0.025	2.90 ± 0.40
3511			0.120 ± 0.018	
3552	$\frac{7}{2}^-$	[12]	0.060 ± 0.008	3.23 ± 0.43
3715	$\frac{5}{2}^+$	[12, 29, 31]	0.086 ± 0.015	2.93 ± 0.51
3846	$\frac{5}{2}^+$	[29, 31]	0.049 ± 0.009	1.78 ± 0.32
3863	$\frac{5}{2}^+$	[12]	0.075 ± 0.011	2.74 ± 0.40
3993	$\frac{3}{2}^-$	[12]	0.119 ± 0.017	2.40 ± 0.34
4018			0.165 ± 0.030	
4173	$\frac{3}{2}^-$	[12]	0.095 ± 0.010	2.03 ± 0.21

TABLE 9

Relative level population intensities and strength functions for ^{90}Zr

Level energy E_k (keV)	J^π	Ref.	Relative intensities I/I_0	f_{kl} (10^{-8} MeV^{-3})
0	0^+	[33–35]	1.000 ± 0.020	11.5 ± 0.23
1762	0^+	[33–35]	0.380 ± 0.012	7.35 ± 0.23
2187	2^+	[33–35]	0.560 ± 0.021	5.71 ± 0.21
2748	3^-	[33–35]	0.130 ± 0.011	4.40 ± 0.37
3081	4^+	[33–35]	0.050 ± 0.009	6.38 ± 1.15
3308	2^+	[33–35]	0.270 ± 0.017	4.13 ± 0.26
3842	2^+	[33–35]	0.180 ± 0.015	3.35 ± 0.35
4126	0^+	[33–35]	0.090 ± 0.013	4.20 ± 0.61
4233	2^+	[33]	0.250 ± 0.014	5.59 ± 0.31
4424	0^+	[35]	0.050 ± 0.012	2.66 ± 0.64
4581			0.130 ± 0.010	
4681	2^+	[34, 35]	0.090 ± 0.013	2.47 ± 0.36
4992	0^+	[35]	0.030 ± 0.010	2.08 ± 0.69
5095	1^+	[35]	0.100 ± 0.011	2.15 ± 0.24
5108	2^+	[35]	0.080 ± 0.020	2.70 ± 0.67
5187	1^+	[35]	0.100 ± 0.011	2.25 ± 0.25
5308			0.110 ± 0.012	

Target thicknesses were determined by measuring the shift in energy of the $^{27}Al(p, \gamma)^{28}Si$ resonance at $E_p = 0.992$ MeV induced in a bare aluminium target with respect to the same resonance induced in the above-mentioned aluminium target with the isotope layer deposited on it. The results are summarized in table 1.

Measurements of the high-energy γ-spectra were performed using a 37 cm^3 Ge(Li) detector with 3.1 keV resolution at $E_\gamma = 1.3$ MeV. The detector, placed at an angle of 90° to the direction of the proton beam, was separated from the target by a 5.1 g/cm^2 lead plug which absorbed the low-energy γ-rays preventing accidental summation of pulses. Owing to the water cooling applied, currents up to 10 μA could be used without visible damage of the targets.

Energy and efficiency calibrations of the spectrometer were performed by measuring the γ-spectrum of the decay of the well-known $^{27}Al(p, \gamma)$ resonance occuring at 992 keV proton energy [17]. The absolute efficiency calibration was made by measuring the sum line in ^{60}Co decay.

The γ-spectra were measured at proton energies varying in steps of 15–18 keV. The target thicknesses and the energy region covered are given in tables 1 and 2. This means that for each of the seven reactions studied 40–50 high-energy γ-spectra were obtained. By summation of these spectra in the whole proton energy region studied, we could get the intensities of transitions to the particular low-lying levels of the final nucleus averaged over that region and normalized to the intensity of the ground state transition. The determined intensities of high-energy primary γ-transitions are given in tables 3–9. The average cross sections for populating the particular low-lying states have also been estimated for all the reactions studied. The average cross sections for populating the ground state, $\langle \sigma_{p, \gamma_0} \rangle$, are given in table 2.

3. Data analysis and results

The partial radiation width for transitions of multipolarity L and energy E_γ from the group of states λ of energy E_λ to the final state k of energy $E_k = E_\lambda - E_\gamma$ is given by the expression [2])

$$\langle \Gamma_{k,\lambda} \rangle_J = f^J_{k,\lambda}(E_\gamma) E_\gamma^{2L+1} / \rho_J(E_\lambda), \tag{2}$$

where $\rho_J(E_\lambda)$ is the density of levels with given spin and parity J^π, and $f^J_{k,\lambda}(E_\gamma)$ is the γ-ray strength function for a transition with multipolarity L from the group of states λ of given spin and parity J^π to the final state k.

The γ-ray strength function for E1 transitions can be determined from the photoabsorption cross section [2]):

$$f(E_\gamma) = \tfrac{1}{3}(26 \times 10^{-8}) \frac{\sigma_0 \Gamma^2 E_\gamma}{(E_\gamma^2 - E_0^2)^2 + \Gamma^2 E_\gamma^2} \quad (\mathrm{MeV}^{-3}), \tag{3}$$

where E_0 and Γ are the energy and width of the giant dipole resonance (in MeV), and σ_0 is the photoabsorption cross section at the giant resonance maximum (in mb).

Photonuclear absorption can be described precisely using the function in a form with two Lorentzian curves corresponding to two values of the isospin, $T_< = T_0$ and $T_> = T_0+1$:

$$f(E_\gamma) = f_<(E_\gamma)+f_>(E_\gamma)$$
$$= \tfrac{1}{3}(26\times 10^{-8})\sum_{i=1}^{2}\frac{\sigma_i E_\gamma \Gamma_i^2}{(E_\gamma^2-E_i^2)^2+\Gamma_i^2 E_\gamma^2} \qquad (\mathrm{MeV}^{-3}), \tag{4}$$

where T_0 is the isospin of the ground state. The ratio of the strengths have been obtained by Fallieros and Goulard [36]) as

$$\frac{\int f_>(E_\gamma)\mathrm{d}E_\gamma}{\int f_<(E_\gamma)\mathrm{d}E_\gamma} = \frac{1}{T_0}\frac{1-\frac{3}{2}T_0A^{-2/3}}{1+\frac{3}{2}T_0A^{-2/3}-4T_0(T_0+1)A^{-2}}. \tag{5}$$

The values of the energy splitting of both isospin components is given by the expression [37])

$$E_2-E_1 = 60(T_0+1)/A. \tag{6}$$

It is easily seen that value of the energy splitting of the isospin components is of the same order as the giant resonance width, so both isospin components can easily be separated and identified.

If we neglect the radiative transitions with multipolarities different from E1 and use the Hauser-Feshbach formula, we can write the relationship between the proton capture cross section $\sigma_{\mathrm{p},\gamma k}$ and the γ-ray strength function for electric dipole transitions $f_{k\lambda}(E_\gamma)$ in the form:

$$\sigma_{\mathrm{p},\gamma k} = \frac{\pi\lambda\!\!\!^{-2}}{2(2I+1)}\sum_{I_c,\, j_p,\, l_p}(2I_c+1)\frac{T_{l_p j_p}2\pi E_\gamma^3 f_{k\lambda}(E_\gamma)}{\sum\limits_{j_{p'},\, l_{p'}} T_{l_{p'},\, j_{p'}}+\sum\limits_{J'}\int_0^{E_\lambda}2\pi\rho_{J'}(E_\lambda-E_\gamma)E_\gamma^3 f_{k\lambda}(E_\gamma)\mathrm{d}E_\gamma}, \tag{7}$$

where $\lambda\!\!\!^-$ is the incident proton wave length divided by 2π; I is the spin of the target nucleus; I_c is the spin of the compound nucleus; j_p and l_p are the spin and orbital momenta of particles in the entrance channel; $j_{p'}$ and $l_{p'}$ are the spin and orbital momenta of particles in the exit channel; $f_{k\lambda}(E_\gamma)$ is the dipole γ-ray strength function for emission of γ-rays from the group of states at energy E_γ to the state lying at E_k (independence of I_c is assumed); $T_{j_p l_p}$ and $T_{j_{p'} l_{p'}}$ are the transmission coefficients for particles in the entrance and exit channels, respectively; $\rho_{J'}(E_\lambda-E_\gamma)$ is the density of levels with spin J' at excitation energy $E = E_\lambda-E_\gamma$.

From expression (7) the intensities of γ-transitions to the particular low-lying states can be calculated directly. This requires, however, assuming a definite shape for the strength function $f_{k\lambda}(E_\gamma)$. The intensity calculated in this way when compared with the results of measurement can be a test of the correctness of the strength function $f_{k\lambda}(E_\gamma)$ used.

The energy dependence of the γ-ray strength function can be determined by analysing the ratio of transition intensities to the chosen j- and k-levels with the same spin and parity J. According to (7) this ratio should be:

$$\frac{\sigma_{\mathrm{p},\gamma_k}}{\sigma_{\mathrm{p},\gamma_j}} = \frac{f_{k,\lambda}(E_{\gamma_k})}{f_{j,\lambda}(E_{\gamma_j})}\left(\frac{E_{\gamma_k}}{E_{\gamma_j}}\right)^3. \tag{8}$$

Assuming that Brink hypothesis holds, i.e. that the condition $f_{k,\lambda}(E_\gamma) = f_{j,\lambda}(E_\gamma)$ is fulfilled for every value k and j, we get from expression (8) the energy dependence of the γ-ray strength function. It deserves noting here that expression (8) can be utilized for determining the strength function from measurements of the cross sections $\sigma_{\mathrm{p},\gamma_k}$ for reactions leading to different levels with the same spin and parity values.

In radiative proton capture studies usually γ-transitions leading to levels with both parities and various spins are registered. To utilize the whole information gathered in the experiment we resort to a procedure which allows us to determine the γ-ray strength function from the intensity of transitions to levels with different spin and parity values. This can be done if we introduce the factor c_{J^π} calculated from the Hauser-Feshbach expression 7):

$$c_{J^\pi} = \frac{\sigma_{\mathrm{p},\gamma_0}(E_\gamma = E_\lambda; J_0^{\pi_0})}{\sigma_{\mathrm{p},\gamma_k}(E_\gamma = E_\lambda; J^\pi)}. \tag{9}$$

The factor c_{J^π} is the ratio of partial cross sections leading to population of the ground state of spin $J_0^{\pi_0}$ and a hypothetical state with spin J^π lying at the energy of the ground state.

TABLE 10

The c_{J^π} coefficients for arsenic and yttrium isotopes

Isotopes	$c_{1/2^-}$	$c_{3/2^-}$	$c_{5/2^-}$	$c_{7/2^-}$	$c_{1/2^+}$	$c_{1/2^+}$	$c_{5/2^+}$	$c_{7/2^+}$	$c_{9/2^+}$
^{71}As	1.29	0.664	1.00	1.20	1.010	0.936	0.841	2.12	3.68
^{73}As	1.47	1.000	2.17	2.86	1.450	1.560	1.850	11.10	13.20
^{75}As	1.23	1.000	4.00	5.26	1.560	1.720	2.310	21.70	23.40
^{85}Y	1.00	0.758	1.63	2.78	0.909	0.847	1.450	7.03	8.11
^{87}Y	1.00	0.862	1.79	2.76	1.340	1.090	2.220	9.17	10.10
^{89}Y	1.00	0.556	1.07	1.82	1.010	0.710	1.070	3.64	6.25

TABLE 11

The c_{J^π} coefficients for ^{90}Zr

c_{0^+}	c_{1^+}	c_{2^+}	c_{4^+}	c_{3^-}
1	0.294	0.458	4.17	1.25

Relation (8), after introducing c_{J^π}, can be expressed as

$$f_{k,\lambda}(E_{\gamma_k}) = c_{J^\pi} f_{0,\lambda}(E_{\gamma_0}) \left(\frac{E_{\gamma_0}}{E_{\gamma_k}}\right)^3 \frac{\langle \sigma_{p,\gamma_k} \rangle}{\langle \sigma_{p,\gamma_0} \rangle}, \qquad (10)$$

where E_{γ_0} and E_{γ_k} are the average energies of γ-transitions to the ground state and

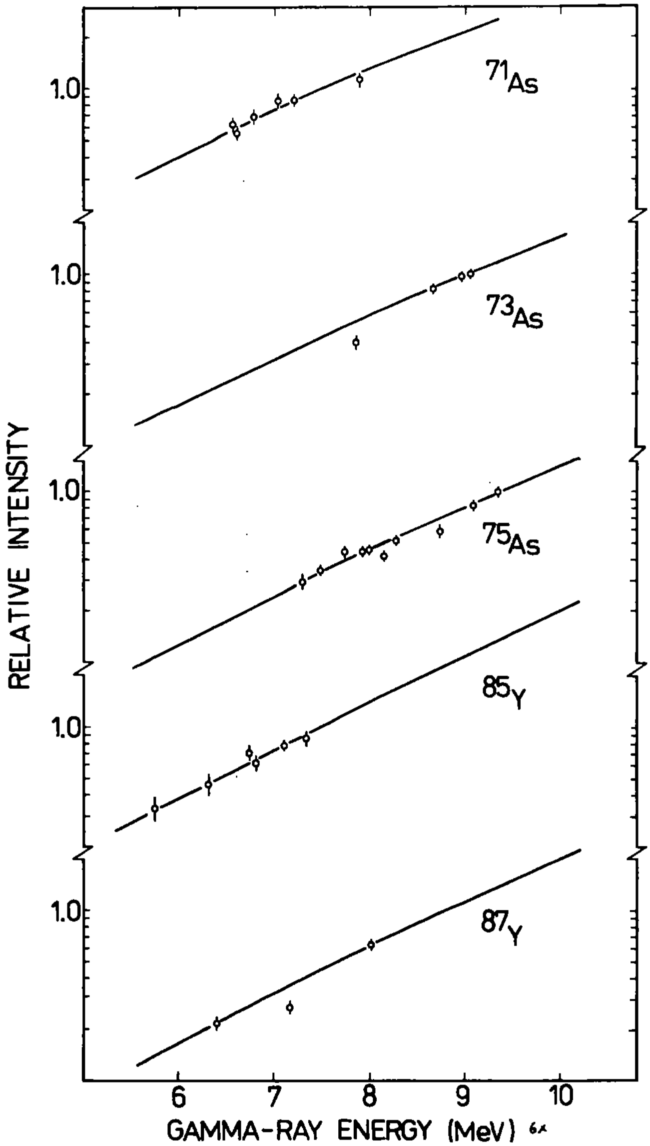

Fig. 1. Relative intensity of transitions to states with spins and parities $\frac{1}{2}^-$ in yttrium and arsenic isotopes. The calculated values (solid lines) and experimental data (open circles) are compared.

the state lying at energy E_k; $\langle\sigma_{p,\gamma_k}\rangle$ and $\langle\sigma_{p,\gamma_0}\rangle$ are the experimental values of cross sections for populating the state of energy E_k and the ground state, respectively; $f_{0,\lambda}(E_{\gamma_0})$ is the γ-ray strength function for the transition to the ground state and $f_{0\lambda}(E_{\gamma_0})$ is at the same time a factor normalizing our results. If we succeed in assigning to $f_{0\lambda}(E_{\gamma_0})$ the value obtained independently in another way, we can determine the absolute values of $f_{k\lambda}(E_\gamma)$. The latter will be burdened with an error

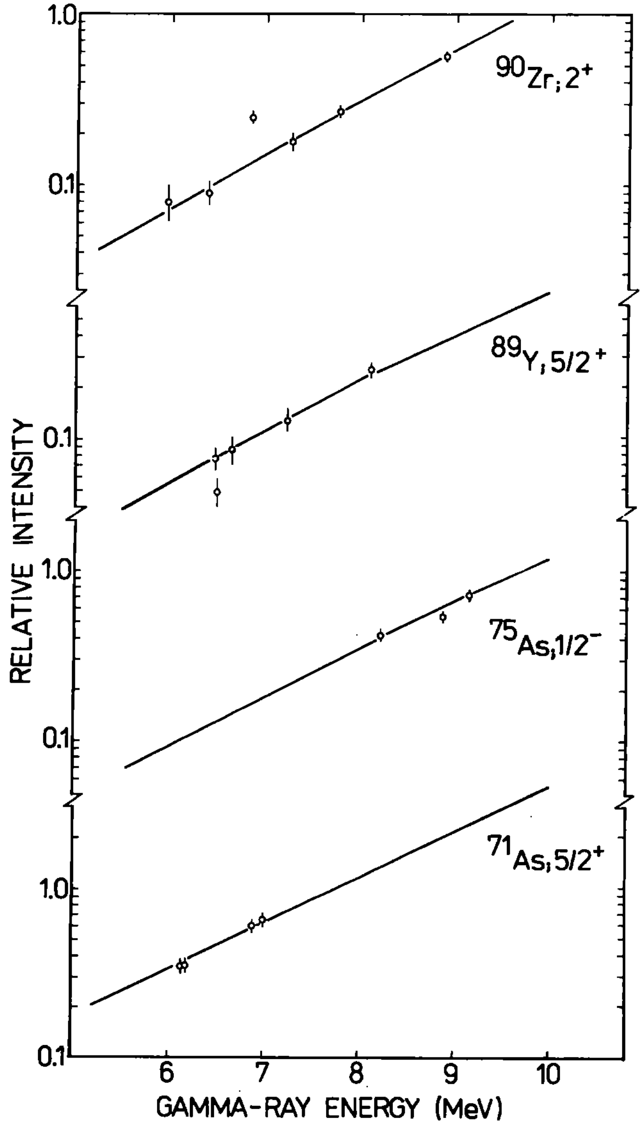

Fig. 2. Relative intensity of transitions to states with selected spin and parity values. The solid lines present the results of calculations and the open circles experimental data.

related both to limited accuracy of determining the relative cross sections and to the error involved in estimating the factor $c_{J\pi}$.

The relative partial cross sections were calculated using formula (7). In these calculations use was made of the proton transmission coefficients obtained from the optical model with the parameters of Becchetti and Greenlees [38]) extrapolated to $E_p = 3$ MeV, the depth of the imaginary potential well being reduced to 6 MeV. In this procedure we used expressions from refs. [39–42]), concerned with investigation of the (p, n) reaction cross sections for nuclei from the mass region 50–80 and at proton energies in the region between 2 and 5 MeV.

In the calculations we used the strength function in the form determined by expression (4). The intensities and the splitting of the isospin components of the giant resonance were calculated from expressions (5) and (6).

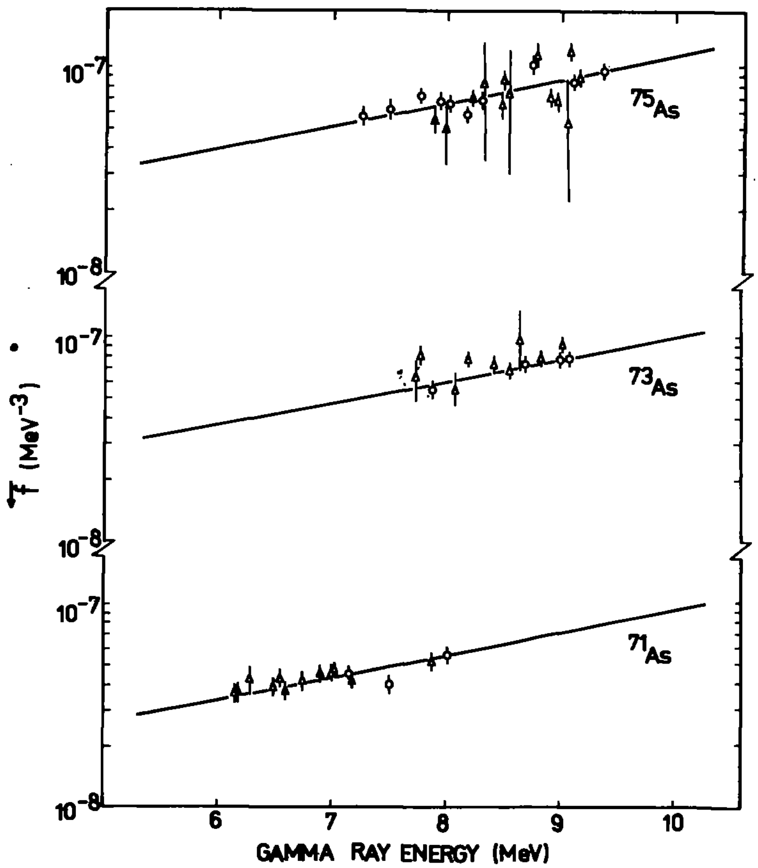

Fig. 3. Gamma-ray strength function for arsenic isotopes. Circles and triangles denote experimental points for levels with spin such as that of the ground state and for levels with spin different from that of the ground state, respectively. The solid lines present the strength function values as described by the Lorentzian curve extrapolated from the giant resonance region.

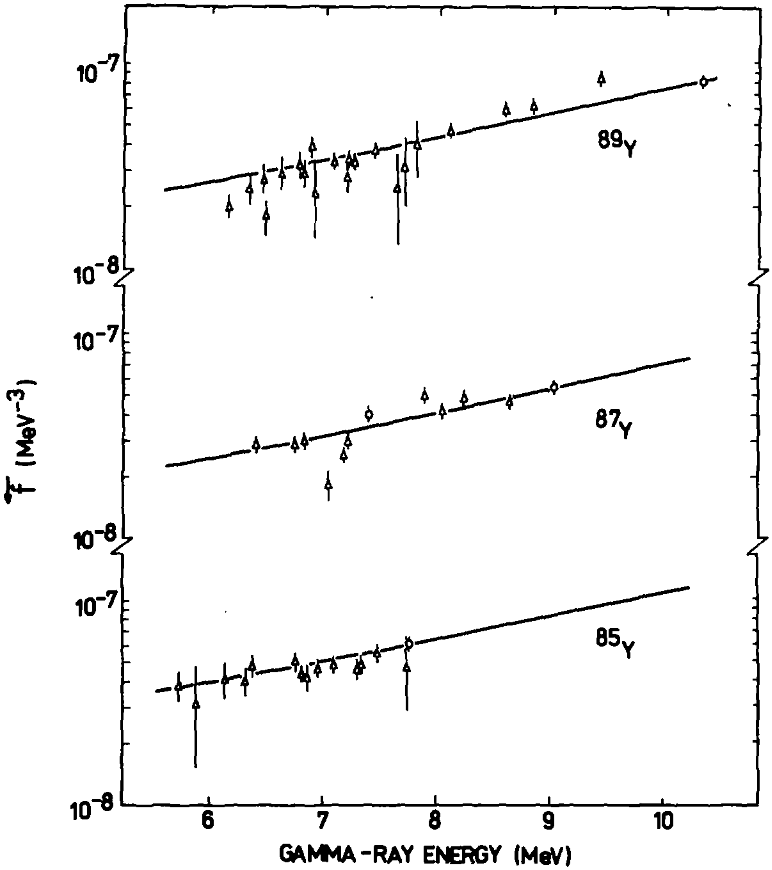

Fig. 4. Gamma-ray strength function for yttrium isotopes. For details see fig. 3.

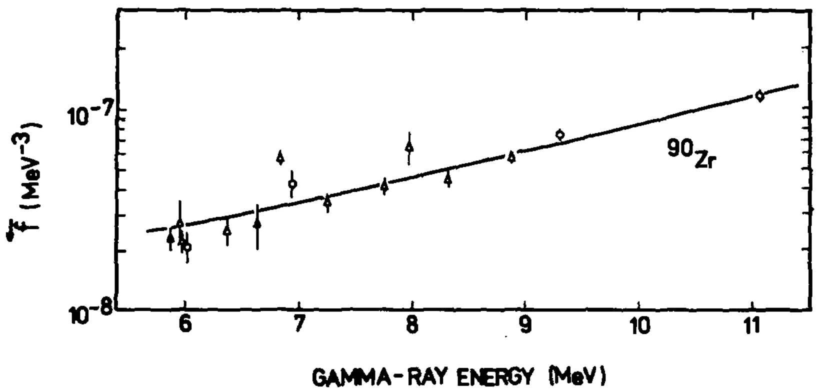

Fig. 5. Gamma-ray strength function for ^{90}Zr. For details see fig. 3.

Since for nuclei from the mass region $A \approx 80$ the total absorption cross section exhausts almost 100 % of the classical sum rule for electric dipole transitions, in the calculations the values of σ_1 and σ_2 fulfilling condition (5) were used.

In figs. 1 and 2 the results of theoretical calculations of relative transition intensities are compared with experimental data. The agreement is satisfactory,

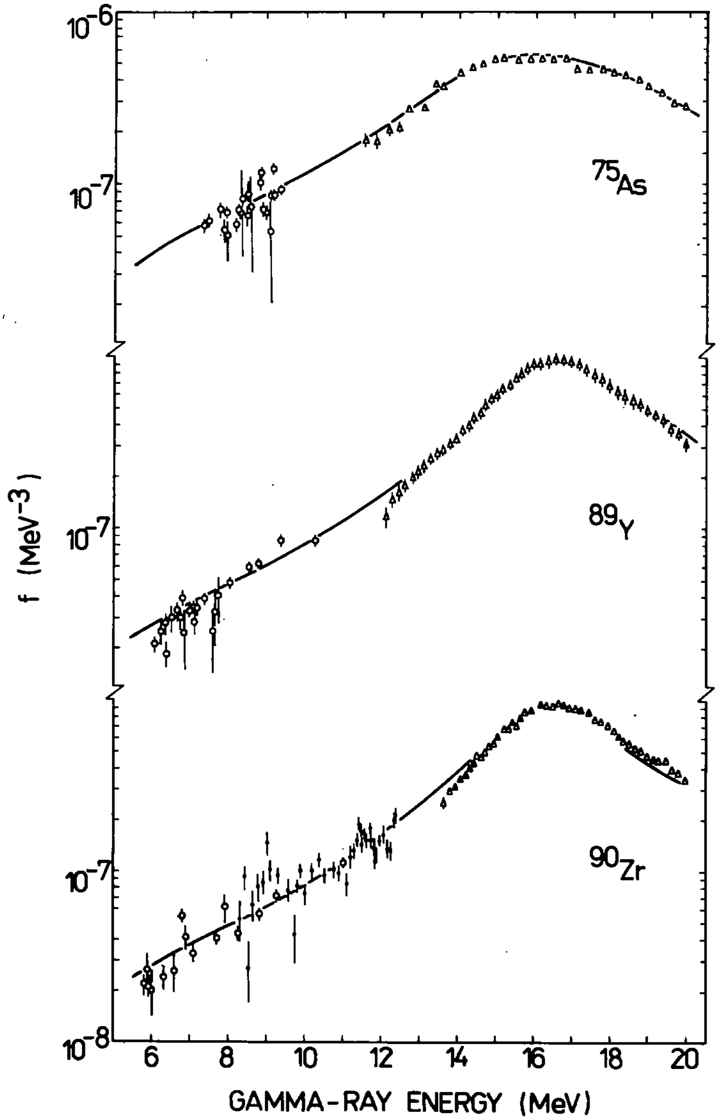

Fig. 6. The strength functions f for ^{75}As, ^{89}Y and ^{90}Zr nuclei. The triangles and black points are from $\sigma_{\gamma n}$ measurements made by Berman *et al.* [43,44]) and Axel *et al.* [45]) respectively. Our results are denoted by open circles. The solid lines are derived from the Lorentzian curve.

which indicates that the assignment of c_{J^π} coefficients is correct. It deserves noting that for clearity we presented in the figures only some selected intensities of transitions to the levels with spins most numerously encountered in final nuclei.

The data concerning the remaining transitions can be found in tables 3–9. The agreement between the calculations and the experimental data is here similar to the cases presented in the figures.

The energy of the levels, shown in the tables 3–9, were evaluated in our experiment with an accuracy of ± 3 keV. The second column of these tables contains the values of J^π taken by us, which were essential to the evaluation of the strength function. The values of J^π were taken, as a rule, from the papers of other authors [18–34]. We used our own values for the spin and parities, evaluated on the bases of the average resonance spectroscopy method [13–15, 35], only when other works did not give us definite value of J^π.

Such a method was used by us because, as already pointed in the introduction, it is possible to evaluate the strength function only in those cases when the values of J^π are precisely known.

When it was impossible to find out precise J^π values for the low-lying levels, the values of the strength function have not been evaluated.

It deserves noting that the calculated absolute cross sections do not agree with experiment so well as the relative ones, and as in other works [11], they are about seven times greater than the experimental cross sections. It should, however, be emphasized that the theoretical calculations were carried out without any free parameters, which explains the observed disagreement between the calculated and measured values of the absolute cross sections.

The values of the γ-ray strength function are presented in figs. 3–5. They were obtained from formulas (4), (9) and (10). The γ-ray strength functions connected with transitions to the ground state and other states of the same spin and parity (and therefore not burdened with errors involved in estimating the factor c_{J^π}) are denoted by open circles. The remaining points, denoted by triangles, relate to cases where $c_{J^\pi} = 1$.

Fig. 6 shows the γ-ray strength functions for ^{75}As, ^{89}Y and ^{90}Zr isotopes. The results above neutron threshold have been calculated by applying eq. (3) to the total γ-absorption cross section reported by Berman *et al.* [43, 44]. For ^{90}Zr we present also the γ-ray strength function calculated on the basis of the total photoabsorption cross section measured below neutron threshold by Axel *et al.* [45].

Our values of the strength function complete other data based on photoabsorption cross section measurements. The substructure observed by Axel *et al.* does not appear in our strength function data. This fact can be explained if we notice that in our experiment the relative intensities were averaged over the energy region of 1.2 MeV, while Axel's measurements have been performed with energy spread of $\approx$ 75 keV.

4. Conclusion

Our experiment indicates that the estimated values of the γ-ray strength function for E1 type transitions to particular low-lying states in all the investigated nuclei lie on the Lorentzian curve extrapolated from the giant resonance region. This supports the thesis that strength functions for successive low-lying states, $f_{k\lambda}(E_\gamma)$, have the same form as that for the ground state, $f_{0\lambda}(E_\gamma)$.

For excited states with spins and parities as in the ground state, we can conclude that strength functions are identical to $f_{0\lambda}(E_\gamma)$. In our experiment we tested the Brink hypothesis for each of the isotopes investigated at one excitation energy E_λ. The values of those energies are listed in table 2. However, a full testing of the Brink hypothesis would require its analysis in a wide range of excitation energies E_λ.

The experiments reported here confirm the assumption, in the energy range investigated 6–10 MeV, that extrapolation of the strength function from the electric dipole giant resonance region is valid.

As the energy dependence of the intensity of primary γ-transitions observed in our experiment is compatible with the strength function for E1 transitions, we are provided with evidence that the contribution of multipole transitions of other types is negligible in the energy and mass region investigated here.

The shape of the strength function in the energy range $E_\gamma < 6$ MeV is still an open problem, and so is the contribution of types of radiation other than E1 in this range. A full explanation of this problem will be possible only after further experimental investigations are made.

The authors would like to express sincere thanks to Dr. J. Piotrowski for his collaboration in the (p, γ) measurements. They are also indebted to the staff of Laboratory EG-5, Institute for Nuclear Research, Dubna, for their valuable assistance.

References

1) C. H. Johnson, Phys. Rev. **C16** (1977) 2238
2) G. A. Bartholomew, E. D. Earle, A. J. Ferguson, J. W. Knowles and A. M. Lone, Adv. Nucl. Phys. **7** (1973) 229
3) R. G. Satchler, Phys. Reports **14** (1974) 97
4) I. Bergqvist, Proc. Int. Conf. on interactions of neutrons with nuclei, ed. E. Sheldon, Univ. of Lowell, Mass, 1976, vol. 1, p. 99
5) P. Axel, Phys. Rev. **126** (1962) 671
6) D. M. Brink, doctoral thesis, Oxford University, 1955
7) V. G. Soloviev, Ch. Stoyanov and V. V. Voronov, Nucl. Phys. **A288** (1977) 376
8) V. G. Soloviev, Ch. Stoyanov and V. V. Voronov, Nucl. Phys. **A304** (1978) 327
9) N. Rosenzweig, Nucl. Phys. **A118** (1968) 650
10) L. M. Bollinger and G. E. Thomas, Phys. Rev. **C2** (1971) 1951
11) P. A. Close and R. C. Bearse, Nucl. Phys. **A201** (1973) 337
12) Z. Wilhelmi, J. Piotrowski, G. Szeflińska and Z. Szefliński, Communication of the Joint Institute for Nuclear Research, JINR, P15-10233, Dubna (1976)

13) Z. Wilhelmi, J. Piotrowski, G. Szeflińska and Z. Szefliński, Communication of the Joint Institute for Nuclear Research, JINR, P15-11640, Dubna (1978)
14) Z. Wilhelmi, J. Piotrowski, G. Szeflińska and Z. Szefliński, Communication of the Joint Institute for Nuclear Research, JINR, P15-11026, Dubna (1977)
15) Z. Wilhelmi, J. Piotrowski, G. Szeflińska and Z. Szefliński, Communication of the Joint Institute for Nuclear Research, JINR, P15-11639, Dubna (1978)
16) C. E. Porter and R. G. Thomas, Phys. Rev. **104** (1956) 483
17) H. L. Scott and T. F. Lusby, Nucl. Instr. **131** (1975) 517
18) R. R. Betts, S. Mordechai, D. J. Pullen, B. Rosner and W. Scholz, Nucl. Phys. **A230** (1974) 235
19) B. Rosner, W. Oelert and L. Shabason, Nucl. Phys. **A256** (1976) 312
20) U. F. von Hundelshausen, Z. Phys. **225** (1969) 125
21) R. D. Mecker and A. B. Tucker, Nucl. Phys. **A157** (1970) 337
22) P. van der Merwe, E. Bernard, J. A. M. de Villiers and J. G. Malau, Nucl. Phys. **A240** (1975) 273
23) M. Schrader, H. Reiss, G. Rosner and H. V. Clapton, Nucl. Phys. **A263** (1976) 193
24) V. Abbondanno, F. Demanins, M. R. Molisson and G. Nardelli, Nucl. Phys. **A305** (1978) 117
25) W. R. Murray, P. J. Celiers and R. Saayman, Nucl. Phys. **A225** (1974) 37
26) L. R. Medsker, G. S. Florey, H. T. Fortune and R. M. Wieland, Phys. Rev. **C12** (1975) 1452
27) J. V. Maher, J. R. Comfort and G. C. Morrison, Phys. Rev. **C3** (1971) 1162
28) R. J. Pelerson and H. Rudolph, Nucl. Phys. **A241** (1975) 253
29) L. Hulstman, H. P. Blok, J. Verburg, J. G. Hoograyling, C. B. Negereveen, H. T. Vijlbvief, E. J. Koptein, S. W. L. Milo and J. Blok, Nucl. Phys. **A251** (1975) 269
30) P. S. Buchman, S. C. Natcher, B. W. Tucker, J. L. Horgan and B. L. Hundepoth, Phys. Rev. **158** (1967) 1041
31) G. Vourvopoulos, S. Shoup and R. A. Brown, Nucl. Phys. **A174** (1971) 581
32) C. J. Umbarger, D. A. Close, W. L. Sievers and R. C. Bearse, Phys. Rev. **C3** (1971) 199
33) R. P. Singhal, S. W. Brain, C. S. Curran, W. A. Gillespie, A. Johnston, E. W. Lees and A. G. Sligth, J. of Phys. **G1** (1975) 558
34) A. B. Tucker and S. O. Simmons, Nucl. Phys. **A156** (1970) 83
35) J. Piotrowski, G. Szeflińska and Z. Szefliński, Communication of the Joint Institute for Nuclear Research, JINR, P15-9455, Dubna (1976)
36) S. Fallieros and B. Goulard, Nucl. Phys. **A147** (1970) 593
37) R. Ö. Akyüz and S. Fallieros, Phys. Rev. Lett. **27** (1971) 1016
38) F. D. Becchetti and G. W. Greenlees, Phys. Rev. **182** (1960) 1180
39) S. Kalias, S. K. Gupta, M. H. Mehta, S. S. Kerekatte, L. V. Namjoshi, N. K. Ganguly and S. Chintalapudi, Phys. Rev. **C12** (1975) 1789
40) C. H. Johnson and R. L. Kernell, Phys. Rev. **C2** (1970) 639
41) C. H. Johnson, R. L. Kernell and S. Ramavataram, Nucl. Phys. **A107** (1968) 21
42) D. P. Balamuth, G. P. Couchell and G. E. Mitchell, Phys. Rev. **170** (1968) 995
43) B. L. Berman, J. J. Caldwell, R. R. Harvey, R. L. Bramblett and S. C. Fultz, Phys. Rev. **162** (1967) 1098
44) B. L. Berman, R. L. Bramblett, J. T. Caldwell, H. S. Davis, M. A. Kelly and S. C. Fultz, Phys. Rev. **177** (1969) 1745
45) P. Axel, K. K. Min and D. C. Sutton, Phys. Rev. **C2** (1970) 689